BREAKTHROUGHS IN LOW-PROFILE LEAKY-WAVE HPM ANTENNAS

Prepared by: Robert A. Koslover

Scientific Applications & Research Associates, Inc.
6300 Gateway Drive
Cypress, CA 90630-4844

15 Dec 2014

Data Item: A001 - Progress, Status, & Management Quarterly Report #5

Prepared for:

Program Officer: Lee Mastroianni
ONR Code 30

OFFICE OF NAVAL RESEARCH
875 North Randolph Street
Suite 1425
Arlington, VA 22203-1995

REPORT DOCUMENTATION PAGE

Form Approved
OMB No. 0704-0188

1. REPORT DATE *(DD-MM-YYYY)*	**2. REPORT TYPE**	**3. DATES COVERED** *(From - To)*
15-12-2014	Quarterly	19 Sep 2014 – 15 Dec 2014

4. TITLE AND SUBTITLE
Breakthroughs in Low-Profile Leaky-Wave HPM Antennas
Progress, Status, & Management Report
(Quarterly Report #5)

5a. CONTRACT NUMBER
N00014-13-C-0352

5b. GRANT NUMBER

5c. PROGRAM ELEMENT NUMBER

6. AUTHOR(S)
Koslover, Robert, A.

5d. PROJECT NUMBER

5e. TASK NUMBER

5f. WORK UNIT NUMBER

7. PERFORMING ORGANIZATION NAME(S) AND ADDRESS(ES)

Scientific Applications &
Research Associates, Inc.
6300 Gateway Drive
Cypress, CA 90630-4844

8. PERFORMING ORGANIZATION REPORT NUMBER

9. SPONSORING / MONITORING AGENCY NAME(S) AND ADDRESS(ES)
Office of Naval Research
875 North Randolph Street
Suite 1425
Arlington, VA 22203-1995

10. SPONSOR/MONITOR'S ACRONYM(S)
Code 30

11. SPONSOR/MONITOR'S REPORT NUMBER(S)

12. DISTRIBUTION / AVAILABILITY STATEMENT
Distribution Statement A. Approved for public release; distribution is unlimited. Other requests for this document shall be referred to the Program Officer listed in the contract.

13. SUPPLEMENTARY NOTES
..

14. ABSTRACT
This report describes progress during the 5th quarter of this program and summarizes the current status of the research. Our primary technical activities this period emphasized the design, analyses, and documentation of representative high-performance FAWSEA and CAWSEA antennas suitable for designation as "standard" or "recommended." The configurations described are scalable with wavelength.

15. SUBJECT TERMS
Leaky-wave Antennas. High Power Microwaves (HPM) Antennas. Low-profile Conformal Antennas.

16. SECURITY CLASSIFICATION OF:			**17. LIMITATION OF ABSTRACT**	**18. NUMBER OF PAGES**	**19a. NAME OF RESPONSIBLE PERSON (Monitor)**
a. REPORT	**b. ABSTRACT**	**c. THIS PAGE**			Lee Mastroianni
Unclassified	Unclassified	Unclassified	SAR	___	**19b. TELEPHONE NUMBER**(incl. area code) (703) 696-3073

Standard Form 298 (Rev. 8-98)
Prescribed by ANSI Std. Z39.18

Table of Contents

List of Figures

1. INTRODUCTION

This is SARA's 5th Quarterly Report for "Breakthroughs in Low-profile Leaky-Wave HPM Antennas," a 37-month Basic Research effort sponsored by the US Office of Naval Research (ONR). This work includes fundamental theoretical analyses, numerical modeling, and related basic research. Objectives include to discover, identify, investigate, characterize, quantify, and document the performance, behavior, and design of innovative High Power Microwave (HPM, GW-class) antennas of the *forward-traveling*, *fast-wave*, *leaky-wave* class.

As planned, in this report we present recommended standard designs for FAWSEA and CAWSEA configurations, which were developed and improved this last quarter. These designs leverage the design methods and rules identified and described in our earlier reports, along with a considerable number of new numerical models to improve them further. We look forward to expanding the family of analyzed/recommended designs to span a much greater variety in the coming months.

1.1. Overview of Previous Activities (1st thru 4th Quarter)

During the *first* quarter, we prepared and established useful equations and algorithms for predicting reflections and transmission of incident TE waves from parallel-wire grills, dielectric windows, and combinations of wire grills with dielectric windows, in problems reducible to purely H-plane (2D) representations. We then applied this theory to guide the design of high-gain configurations (again, limited to 2D, H-plane representations) for linear, forward traveling-wave, leaky-wave antennas. The theory built upon equivalent circuit methods and wave matrix theory, which provided useful formalisms upon which we continue to build.

During the *second* quarter, we pursued initial extensions of the previous work into three dimensions, in order to include phenomena with E-plane dependencies. We succeeded in adding into the wave-matrix formalism the reflection/transmission properties associated with the transition to free space from a *finite-width* leaky-wave channel, including the edge-tapering essential to HPM applications. These geometric aspects do not arise in analyses confined to the H-plane alone. Our 3D analyses were somewhat more reliant on numerical models than in the 2D analyses, due to the greater complexity of identifying and/or building practical analytic approaches capable of addressing true 3D geometries of interest.

During the *third* quarter, we explored channel-to-channel coupling (aka, mutual coupling) which (as we have noted earlier) is an important design concern, since it can impact antenna performance significantly in terms of gain, peak power-handling, and impedance matching. Our approach leveraged mostly numerical methods, along with some intuitive arguments, as we explored designs exhibiting different degrees of mutual coupling between adjacent channels. As past and current antenna literature attest, mutual coupling analyses are non-trivial; suffice to say, there is still much work to be done in this area.

During the *fourth* quarter, we continued to study and employ wave-matrix based methods, but with less success than before in applying this approach to *improve* or *optimize* the initial designs. The formalism itself is still valid, but offers reduced practical rewards once an *initial* (i.e., not fully-optimized) geometry (e.g., grill, window, channel depth, etc.) is derived from the more basic-level principles. At that stage, we are finding that further optimization is currently best proceeding via numerical means. Additional work in the fourth quarter led us to identify *new aperture geometries* of potentially-significant practical value, which included the "BAWSEA" and "GAWSEA". These configurations may significantly extend the utility of leaky-wave antenna technology to support integration on more challenging platforms.

For more information, we encourage the reader to refer our earlier *Quarterly Reports #1* thru *#4.*

1.2. Overview of Recent Activities (5th Quarter)

As planned for this quarter, we applied the theoretical tools and methods identified and/or developed during the first year of this program to improve upon our earlier approaches to design and optimization of specific leaky-wave HPM-capable antennas. We have now generated and documented some specific scalable examples of high-performing FAWSEAs and CAWSEAs in this report and plan to document others in the near future.

Section 3 describes the technical work mentioned above in more detail.

2. STATUS OF THE PLAN/SCHEDULE AND FUNDING

Figure 1 (next page) maps out the updated program plan, for quick reference. As of the time of this report, in regard to the analyses tasks (Tasks {2.x}), we are now shifting attention toward Tasks 2.3 and 2.4. The "standard" designs for FAWSEA and compensated CAWSEA described in this report, which offer excellent performance characteristics, were developed and documented under Tasks 3.1 and 3.2. Additional versions (to span a range of aspect ratios and curvatures) along with updates to these standard designs are planned, as well as attending to AWWSEA and RAWSEA variants, in the coming months.

The subject contract was awarded on 9/18/2013 and has an end date of 10/17/2016. The total contract value is $868,350, with current (per P00003 signed on 4/24/2014) allotted funding of $406,530. According to SARA's accounting system, as of Dec. 12, 2014, expenses (including fee) have totaled $351,500, thus leaving $55,030 available. If one simply compares the calendar and spending on this project, we have consumed ~40% of both the calendar and contract value.

Remaining allotted funds should last approximately two more months, at the current rate of work. This is fully-consistent with ONR's estimate in P00003 that the allotted amount would "cover the period from date of award through seventeen (17) months." We thank ONR for the support to date and encourage ONR to provide additional incremental funds within the next two months, to maintain program progress/continuity.

There are no technical, schedule, or other funding-related program problems/concerns to report at this time.

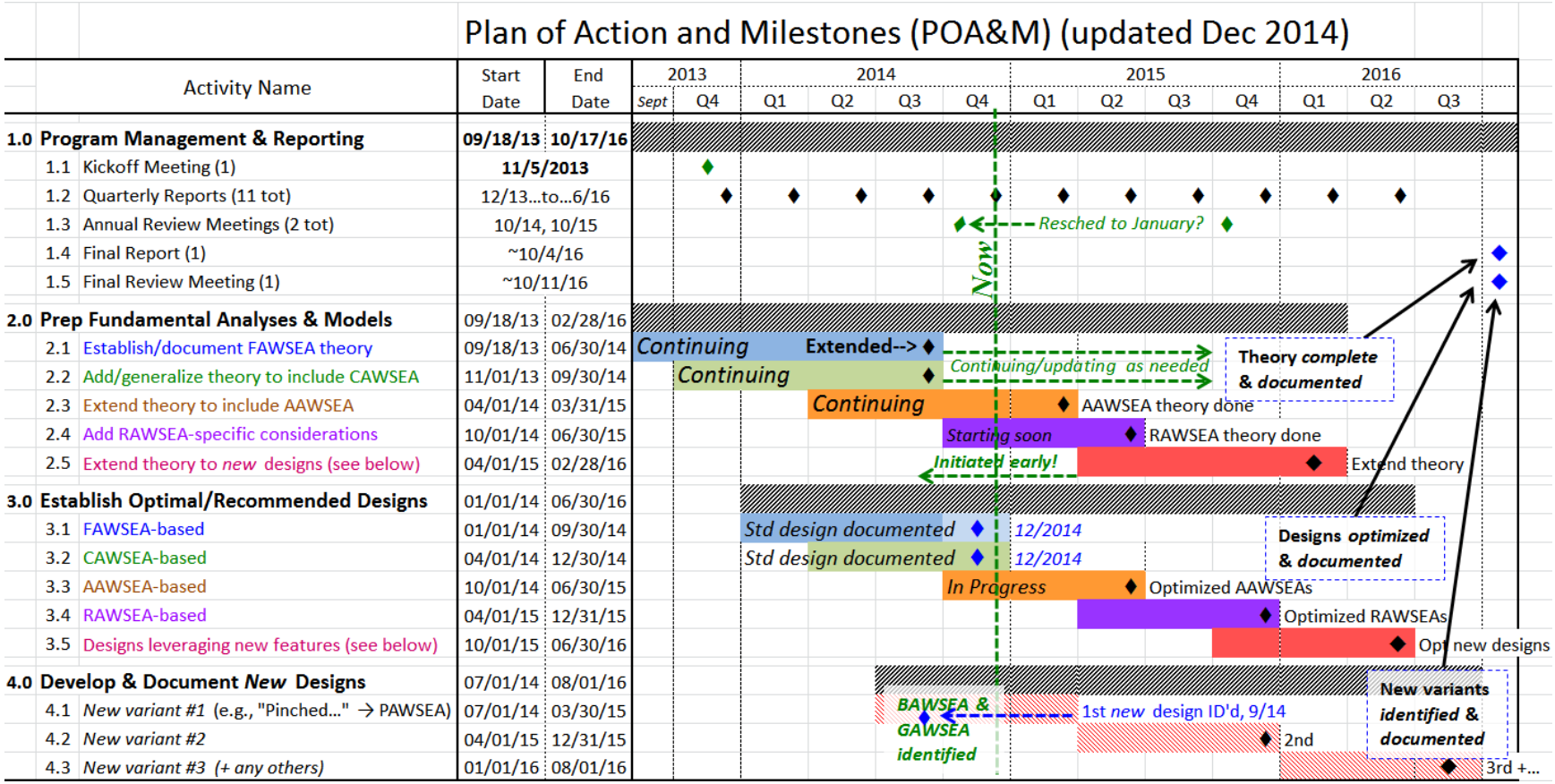

Figure 1. Updated Program Plan

3. RESEARCH PERFORMED THIS PERIOD

Descriptions of recommended high-performance FAWSEA and CAWSEA designs are provided in the sections below. The designs described here were developed and sized for f_0=1.0 GHz; their dimensions may be scaled linearly (all components, isotropically) proportional to λ_0, to support other RF/microwave frequencies. Geometries are presented first, in Sections 3.1-3.3, in a level of detail sufficient (or nearly sufficient) to guide preparation of fabrication-level drawings by a mechanical engineer possessing basic familiarity with HPM-capable antennas. Key features of the *single-channel* FAWSEA design (channel depth, channel width, wire sizes, wire spacing, and tapering along the length) are also used in both the 4-channel FAWSEA and 4-channel CAWSEAs described here. However, in the CAWSEA, the channels are oriented radially rather than parallel, and there is additional curvature/ shaping to the structures near and in the aperture region, otherwise not present in the FAWSEA. The aperture window is polyethylene, with ε_r taken equal to 2.26. The window is deliberately-shaped to allow O-rings (silicone recommended, due to microwave compatibility) to be included around the window edges to provide the vacuum seal. Additional O-ring material is used in strips between the channels, along where the window also makes contact with interior metal parts of the aperture. High peak power (e.g., GW-class) operation requires that the antenna be evacuated. A vacuum at 10^{-6} Torr or better is sufficient to ensure proper insulation. This is readily achievable via commercial vacuum pumps. Predicted performance characteristics of these designs are presented in Section 3.4. Figure 2 introduces the geometries of the antennas.

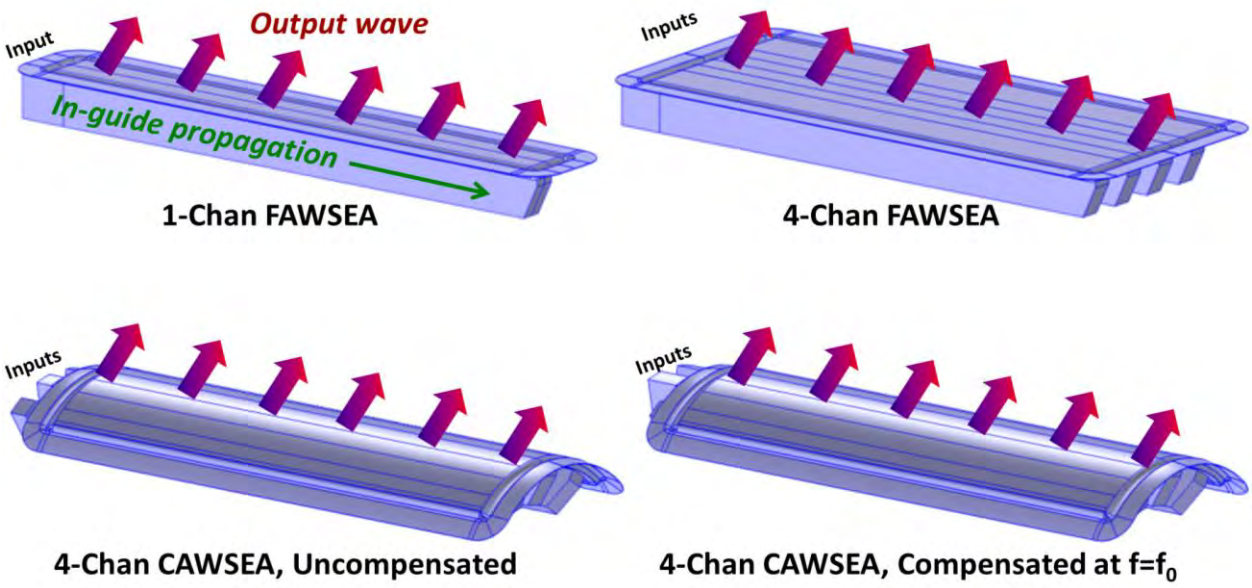

Figure 2. Perspective views of the subject antennas. Each is described in much more detail in the subsections that follow.

3.1. Geometry, Single-Channel FAWSEA

Figure 3 shows the cross-section of the single-channel FAWSEA, in a slice just past where the evacuated channel joins to a rectangular waveguide input feed. The geometry connection can be understood better in conjunction with the side view in Figure 4. In Figure 3, The downward-folds of the window lead into a conducting "well" where they rest on the O-ring channels along the left and right edges. The heavily-rounded edges at the top of the channel and the rising parts of the wings form the sides of this "well", which dramatically suppresses the electric fields at the triple-junction region where air, insulator, and conductors all come together. This is an important HPM-enabling feature of the design, since triple-junctions in high-field locations are well known for serving as initiation points for surface breakdown.

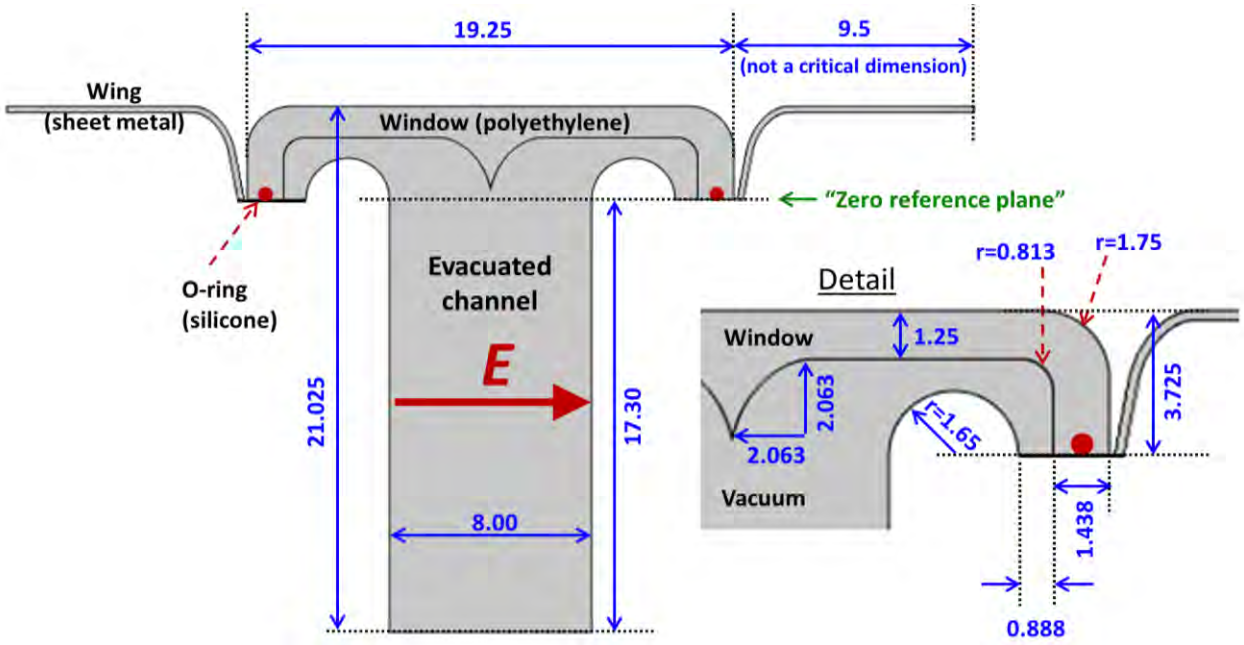

Figure 3. Single FAWSEA channel, cross-section taken at junction to feed. Units are cm.

The leaky-wave grill is a plane-parallel array of 36 wires that are equally-spaced at center-to-center separations of 5.25 cm, beginning (with Wire #1) at 5.25 cm from where the aperture joins to the feeding waveguide. Per Figure 4, this plane of wire-centers is positioned 9.1 mm below the "zero reference plane" noted in Figure 3. The radii of these wires are listed in Figure 5.

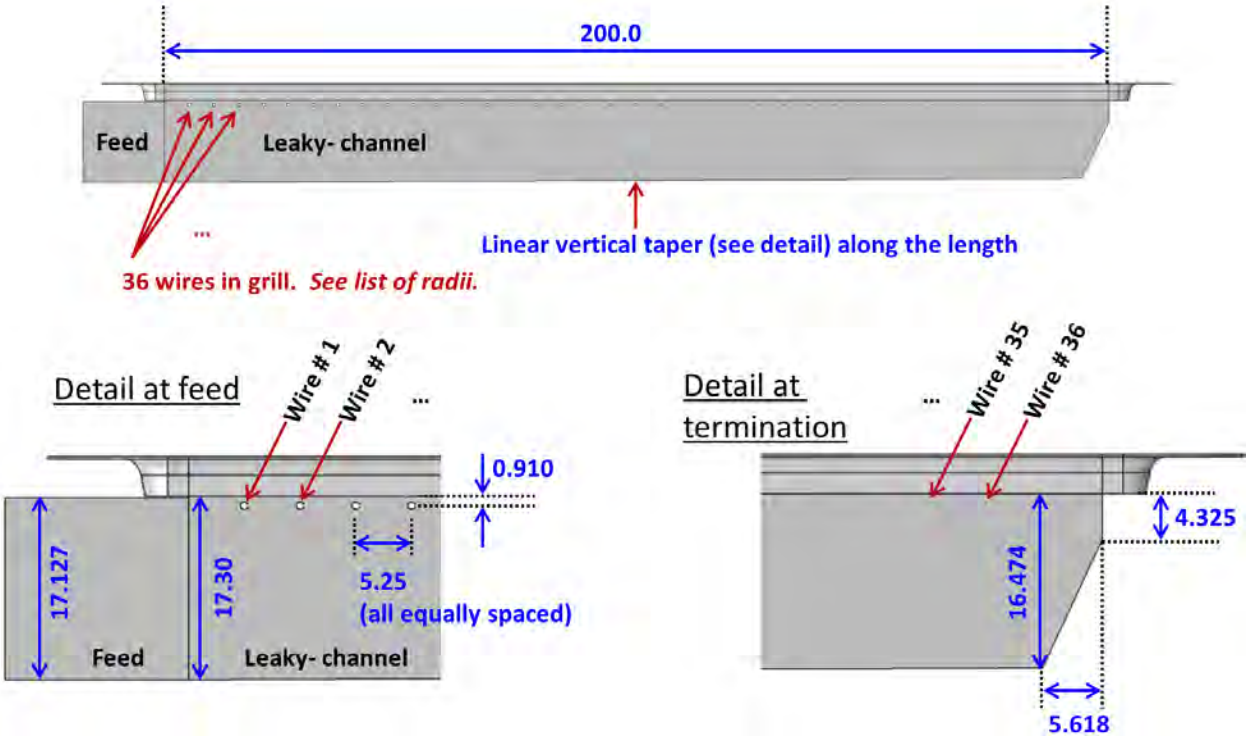

Figure 4. Single channel side view, including wires and tapered backplane. Units are cm.

The wire radii in Figure 5 were derived via methods described in our earlier reports. The last two wires in the list (#'s 35 and 36) are thicker (and match #34) than those that arise from the analyses, to facilitate more practical and rugged fabrication, while ultra-thin wire #'s 37 and 38 (not listed) were simply dropped altogether. The channel is linearly-tapered in depth relative to the "zero reference plane" (note the shallower depth at the termination end vs. at the feed end, as shown in the details in Figure 4) to improve performance by maintaining nearly constant wave phase velocity in the channel, increasing the gain, and reducing the VSWR. The initial taper from feed to termination was set based on an expression for the effective penetration of a reflected wave from a wire grill (as reported in our earlier work), subsequently modified based on results of 3D models, to yield better performance.

Wire #	Radius (mm)		Wire #	Radius (mm)
1	3.505		19	2.361
2	3.459		20	2.268
3	3.412		21	2.171
4	3.362		22	2.068
5	3.312		23	1.959
6	3.260		24	1.843
7	3.205		25	1.721
8	3.149		26	1.592
9	3.091		27	1.453
10	3.031		28	1.306
11	2.968		29	1.150
12	2.903		30	0.983
13	2.835		31	0.806
14	2.765		32	0.620
15	2.691		33	0.430
16	2.614		34	0.245
17	2.534		35	0.245
18	2.450		36	0.245

Figure 5. List of wire radii vs. position index. Wire spacing is fixed at 5.25 cm, center-to-center. All 36 wires are parallel and lie in the same plane, 9.1 mm below the "zero-reference plane" in Figure 3.

Due to left-right symmetry, full numerical RF models of all the antennas in Figure 2 can be made using only half of each antenna, which helps speed-up the computations. Figure 6 shows two views of a half-single channel, from one of our 3D models. Note the wrap-around nature of both the O-ring well and wing, the latter which would generally meld smoothly onto a larger conducting surface, if the aperture were attached all around to a supporting mount.

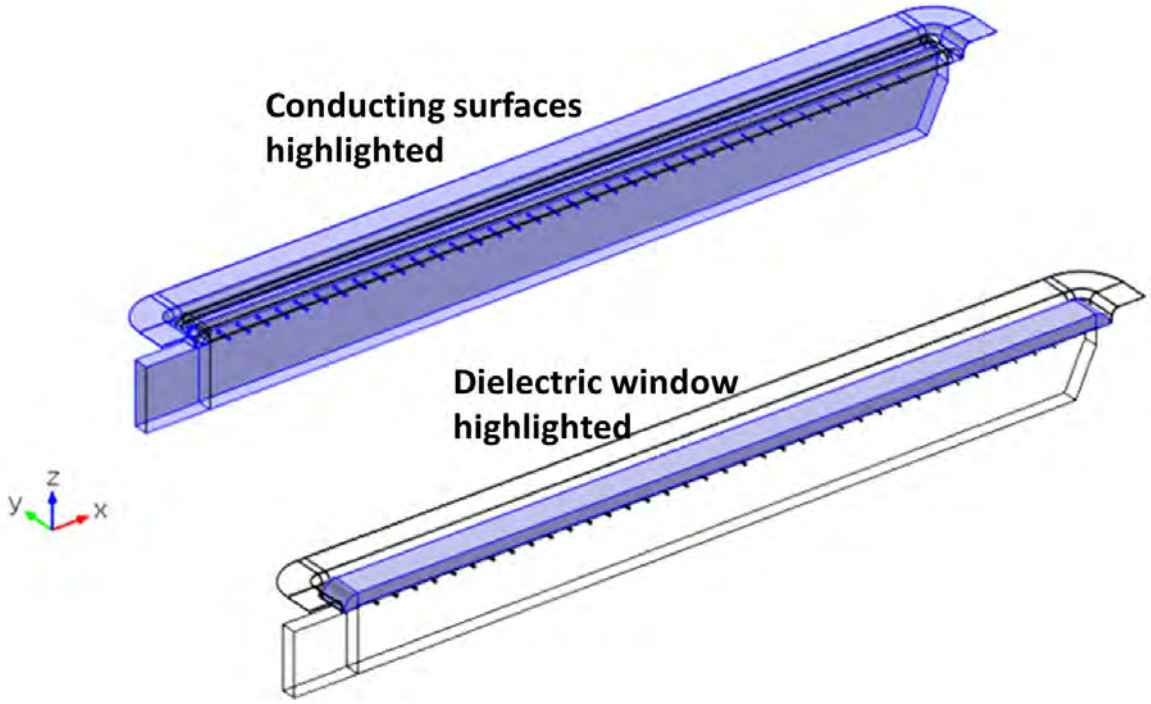

Figure 6. A half-channel, sliced along its symmetry plane for use in 3D RF modeling.

Single-channel FAWSEAs may have some direct applications, but we are more interested in their role as building blocks in constructing more general multi-channel FAWSEA and CAWSEA antennas.

3.2. Geometry, 4-Channel FAWSEA

Figure 7 shows the cross-section of a four-channel FAWSEA based on the single-channel FAWSEA described just above. We found that four 8cm-wide channels with a c-to-c separation of 19 cm yield very good performance in terms of aperture efficiency and control of cross-channel coupling. Figure 8 shows two views of a half 4-channel FAWSEA, from one of our 3D models.

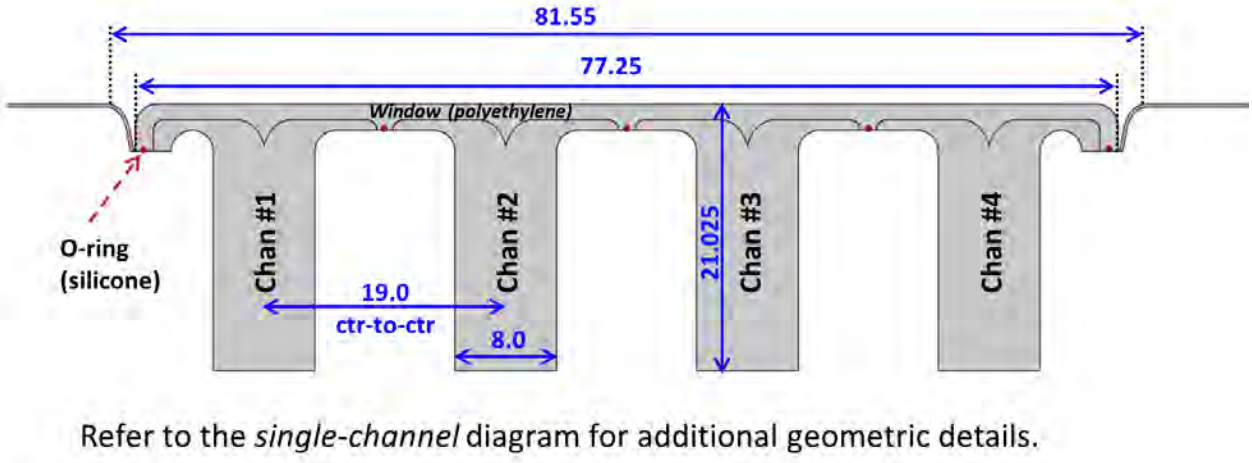

Figure 7. Four channel FAWSEA cross-section (not tapered). Units are cm.

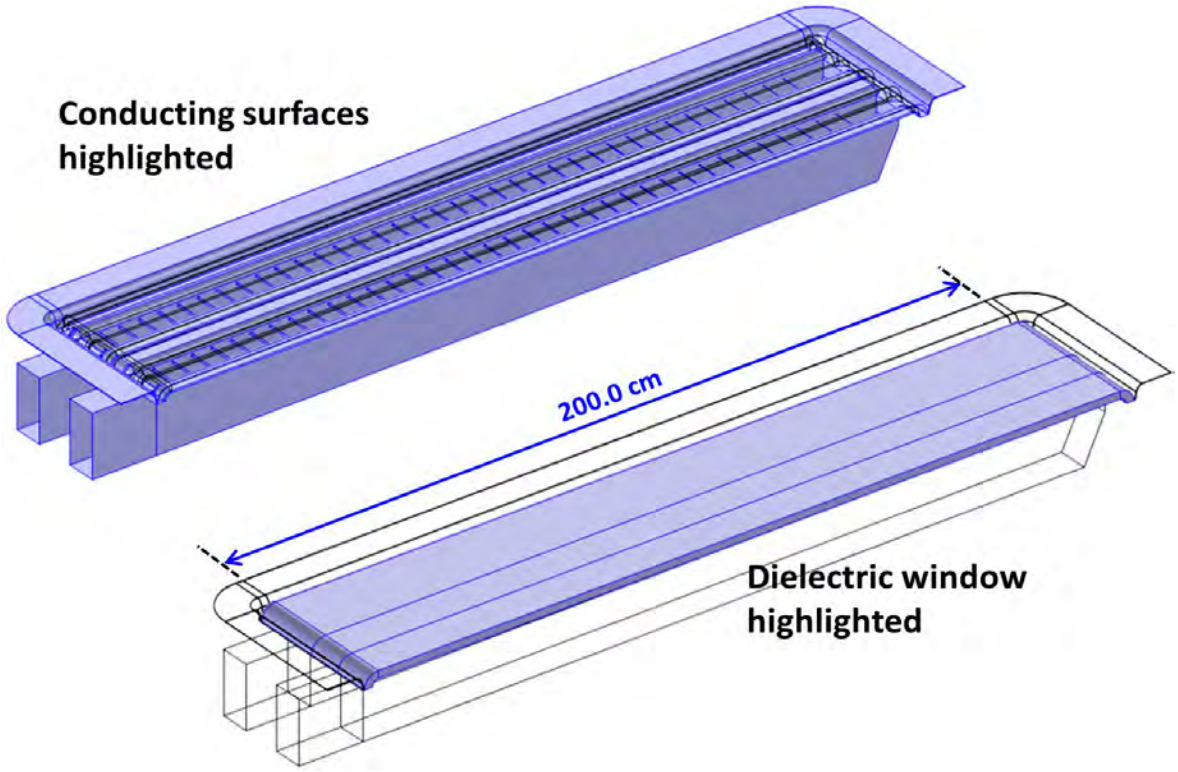

Figure 8. Half of a 4-chan FAWSEA sliced along its symmetry plane, for 3D RF modeling.

3.3. Geometry, 4-Channel CAWSEA

The four-channel CAWSEA in Figure 9 is likewise derived from the single-channel and four-channel FAWSEA design. Extending the feed guides to the center channels (see Figure 10) compensates, in part, for the aperture-curvature induced phase error (and the decrease in gain) that would otherwise occur.

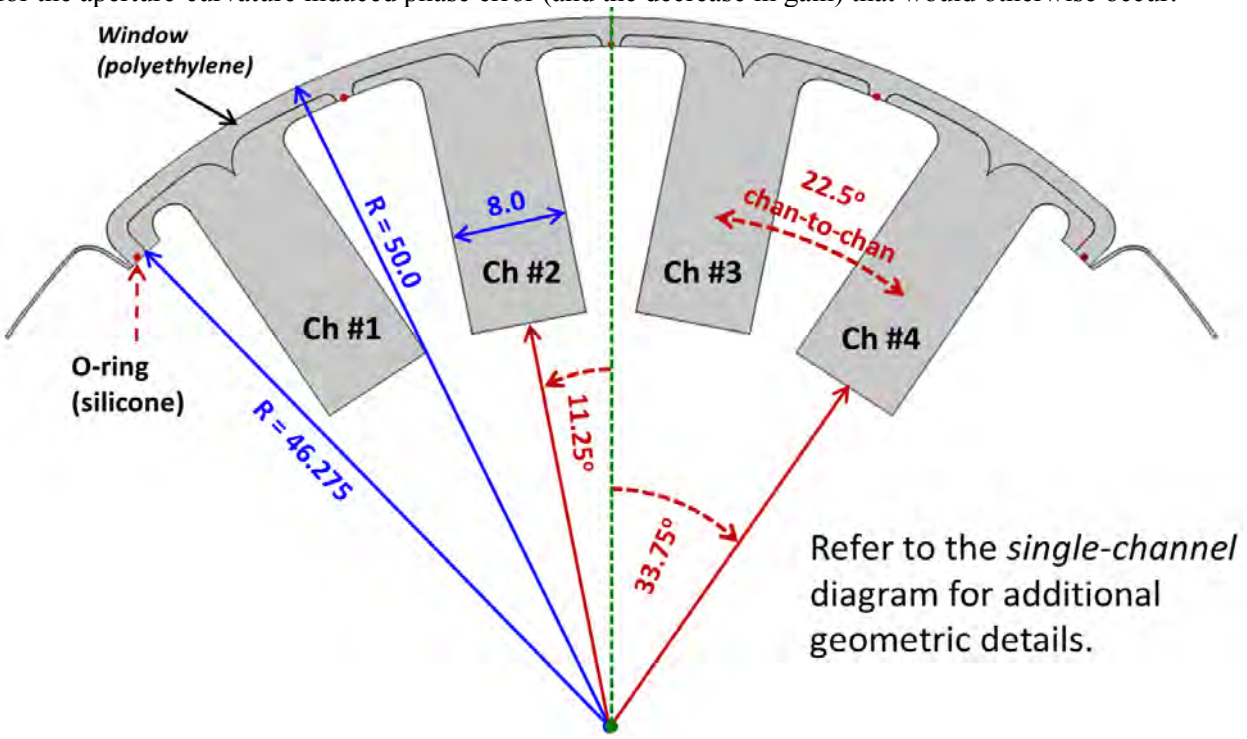

Figure 9. Four channel CAWSEA cross-section (not tapered). Units are cm.

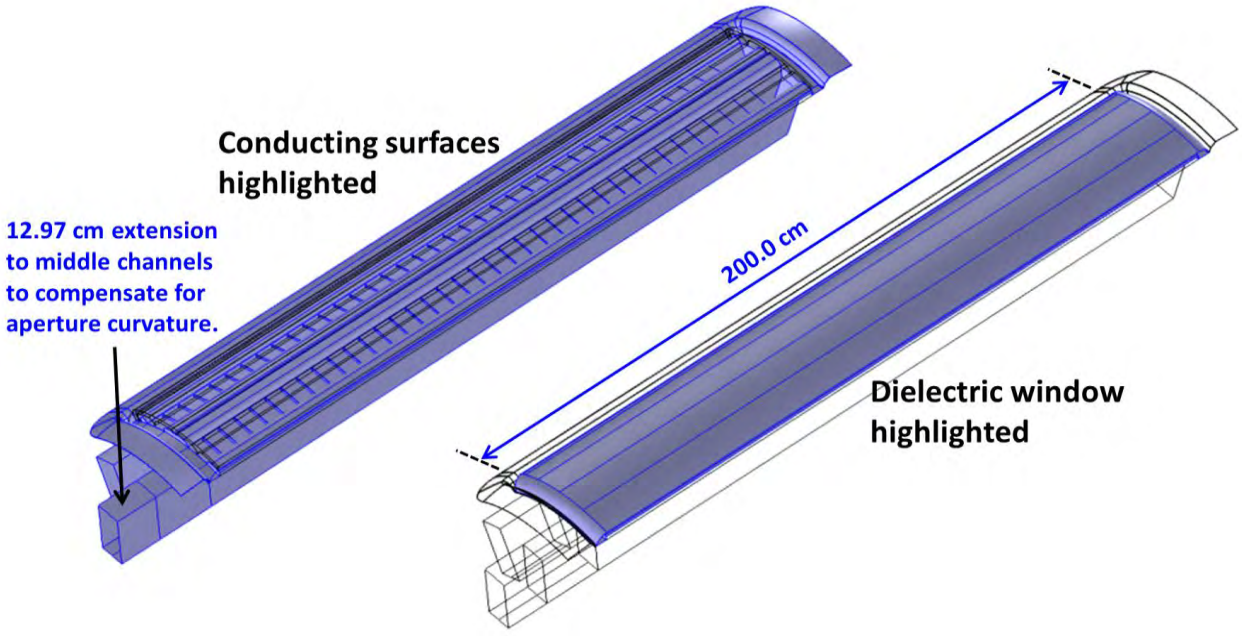

Figure 10. Half of a 4-channel, compensated CAWSEA, sliced along its symmetry plane.

3.4. Predicted Performance Characteristics

Predicted performance characteristics the aforementioned antennas are described below. In addition, we will contrast some of the performance characteristics of the compensated CAWSEA (i.e., including the waveguide extension in Figure 10) with an uncompensated version.

The computed effective[1] VSWR for the aforementioned antennas is plotted in Figure 11. All are very good across a +/-10% bandwidth around f_0. In this case, we found minimal differences in the VSWRs comparing the compensated and uncompensated versions of the CAWSEA, so only the former is shown in Figure 11. In contrast, substantial differences are observed in the gains, as noted in Figure 12.

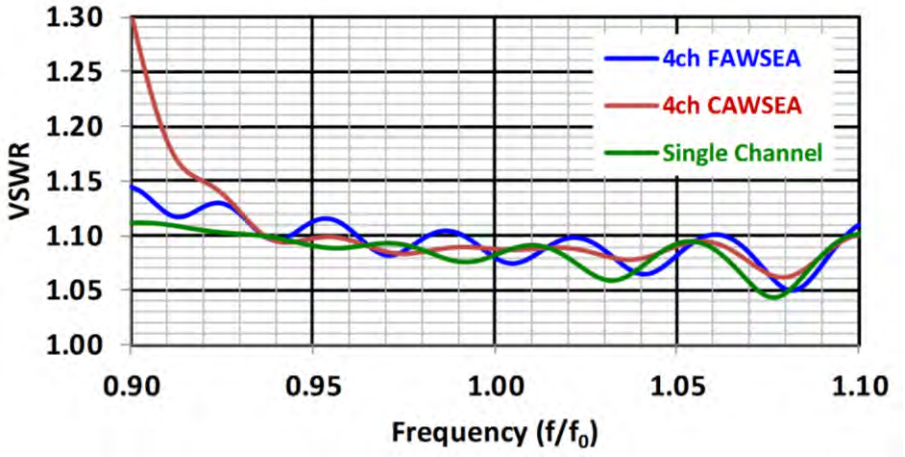

Figure 11. Computed Effective VSWR vs. Frequency

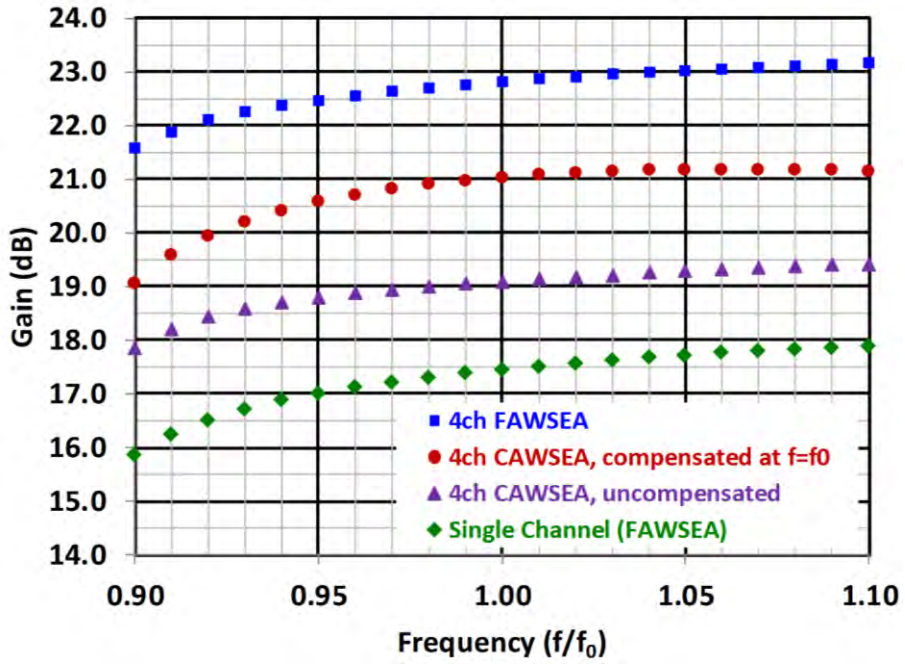

Figure 12. Computed Gain vs. Frequency

[1] In the case of multiple channels, the *effective* VSWR is extracted from the overall forward and reflected powers.

The computed gains of these antennas may perhaps be better appreciated when considered in the context of *aperture efficiency*. To compute this quantity properly for the 4-channel FAWSEA, we need an *unambiguous* definition of the "geometric area" of the aperture, but this is not immediately obvious by inspection, due to the presence (and helpful impact upon RF performance) of the "wings." Excluding the wings entirely from the assumed geometric area would lead us to overestimate aperture efficiency, but it would also be a mistake to include their *full* extent, since they are of somewhat arbitrary size (and may be considered, at least partially, as surrogate extensions of a platform on which such an antenna aperture might be integrated). An unambiguous resolution was attained by defining the "geometric" area of the aperture via a separate 3D numerical RF calculation (not shown here) in which we *replaced* all the FAWSEA channels and window with an *idealized flat rectangular aperture* across which we imposed computationally a 100%-uniform E-field, located in the "zero reference plane," while surrounding it by the *same wings* as shown in Figure 8. This computation allowed us to extract (from the performance of this idealized-aperture case) a value of the geometric area = 1.677 m^2, which (as expected, due to the beneficial effects of the wings) is somewhat *larger* (by ~4.6%) than the window's *physical* projected area (~1.603 m^2). In essence, this way of computing aperture efficiency for the 4-channel FAWSEA (and CAWSEA) compares computed gain to that from an ideal uniform-field aperture *bordered by the same wings*. This definition, in combination with the gains computed earlier, promptly yields Figure 13.

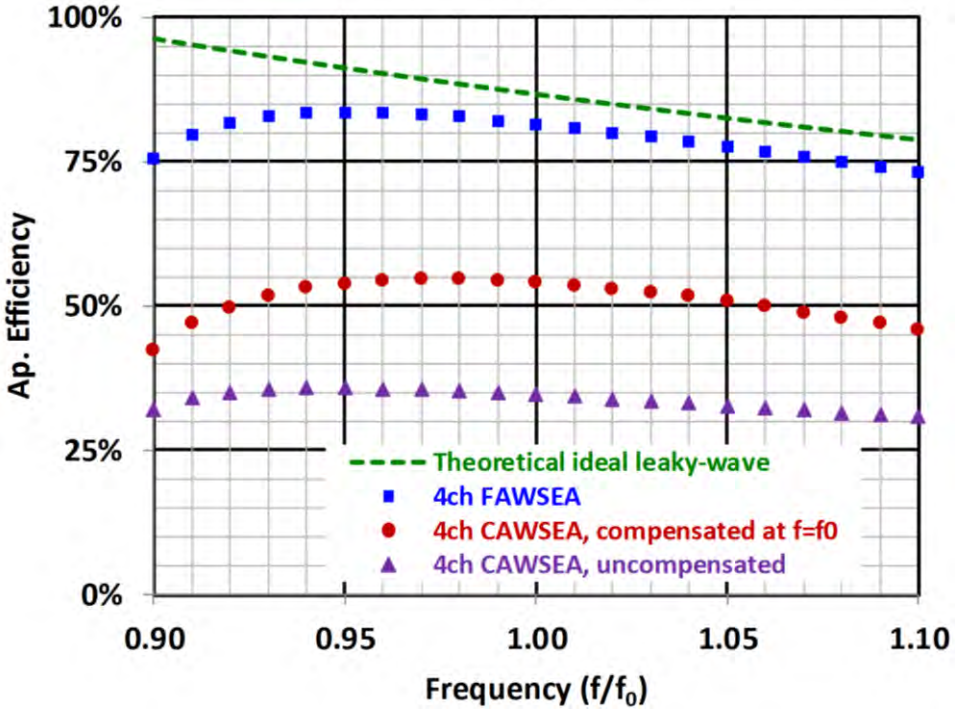

Figure 13. Predicted Aperture Efficiency vs. Frequency.

Note the theoretical upper-bound based on the ideal *leaky-wave* aperture efficiency (shown via the green dotted line) is always less than 100% because the beam is *tilted*. It corresponds simply to $\cos(\theta_b)$, where θ_b is the angle of the beam relative to the aperture normal. The predicted realizable aperture efficiency of the 4-channel FAWSEA (blue squares in Figure 13) is unquestionably excellent. The aperture efficiency of the *compensated* CAWSEA is not as high, but still respectable, and exceeds 50% over a considerable bandwidth. In contrast, the aperture efficiency of the *uncompensated* CAWSEA suffers all the classic consequences of entirely-uncorrected aperture curvature. One can also assess the (related) channel arraying efficiency by comparing the curves in Figure 12. *Ideally*, arraying four channels would deliver +6.02 dB more gain than a single channel alone. At $f=f_0$, the 4-channel FAWSEA, compensated CAWSEA, and uncompensated CAWSEA yield increases in gain of +5.36dB, +3.58dB, and +1.64dB, respectively, over that of a single channel.

Figure 14 shows phase-snapshots of surface electric fields on the windows of uncompensated vs. compensated CAWSEAs (half-models shown).

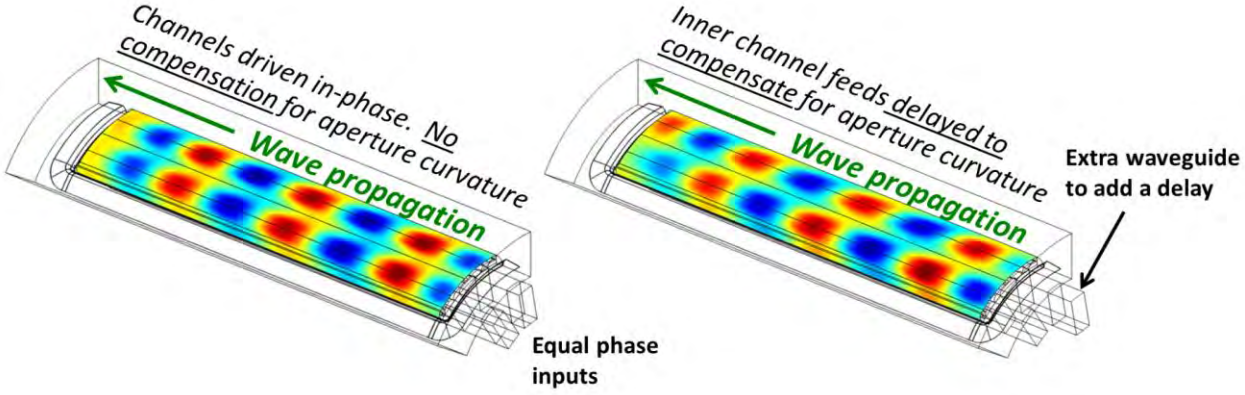

Figure 14. Aperture E on an uncompensated (left) vs. compensated (right) CAWSEA at f_0.

Fortunately, the "shear" introduced to the aperture field distribution on the surface of the compensated CAWSEA does not appear to yield troublesome "hot-spots" that might encourage breakdown. Figure 15 shows[2] predicted peak electric field values on the exterior aperture surfaces for the 4-channel FAWSEA and both CAWSEAs vs. frequency, corresponding to a total input power of 1.0 GW (i.e., 250MW per channel) For more than half of the frequency range, the compensated CAWSEA's peak surface fields are actually less than those in the uncompensated configuration.

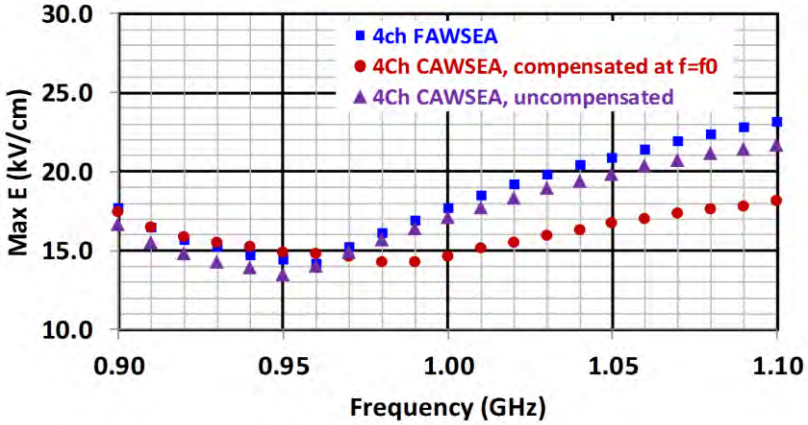

Figure 15. Peak values of E_{max} vs. frequency on exposed exterior window surfaces, for total input power = 1 GW.

For all the designs presented here, the beam tilt vs. frequency follows closely to the theoretical value of $\theta_b = \cos^{-1}(f_c/f)$, where f_c is the effective cutoff frequency of a leaky-wave channel. For the case where f_0 =1.0 GHz and θ_b (by design) is 30°, the value of f_c = 866 MHz. Beam tilt found from a model of the 4-channel FAWSEA vs. this theoretical curve is shown in Figure 16. Results for the other antennas closely track the same curve.

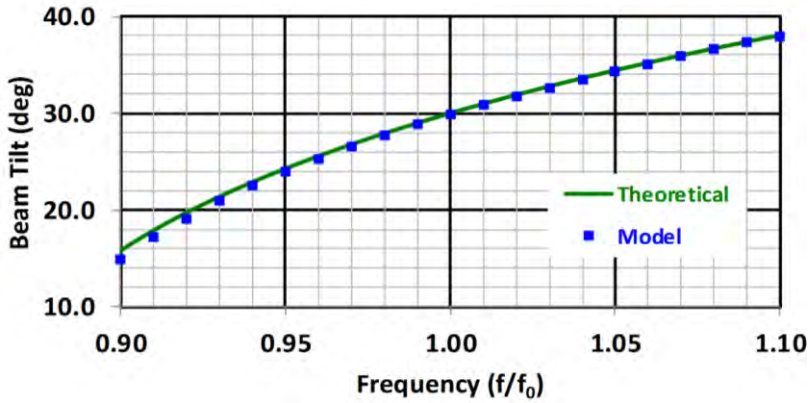

Figure 16. Predicted beam tilt relative to aperture normal, vs. frequency.

[2] If scaling designs presented here to other center (f_0) frequencies, the field values in Figure 15 (with P_{in}=1 GW held fixed) scale proportional to $(f_{0,new}/1.0\ GHz)^2$. In general for HPM, strive to keep E_{max} < 30 kV/cm on the exterior.

Principal-plane polar far-field pattern cuts for the subject antennas at $f=f_0$ are shown in Figure 17. The E-plane cuts (shown in red) are at a 30° angle relative to the aperture normal, so as to slice through the beam peak, and appear centered on 90° in the figures. The H-plane cuts (shown in blue) exhibit the as-designed beam tilt of 30° relative to the aperture normal. Note how the beamwidths in the H-plane are all about the same (corresponding to the in-common aperture length) while the E-plane beamwidths vary markedly, due to either: (a) 1 channel vs. 4 channels, or (b) the effective phase uniformity in the plane-projected aperture field distribution, looking across the narrower dimension of the antenna. (Once again, a comparison of the uncompensated vs. compensated versions of the CAWSEA is instructive.)

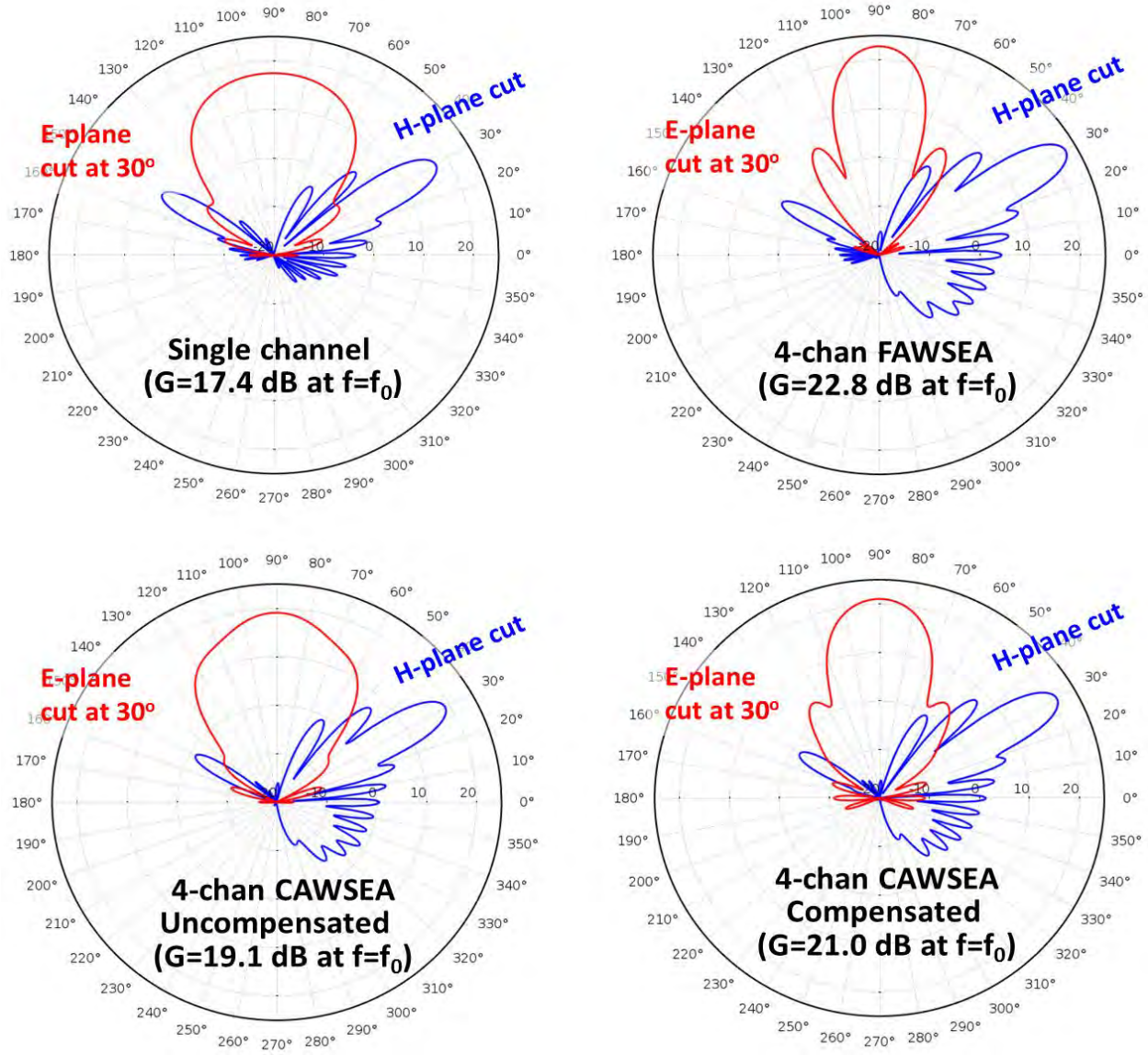

Figure 17. Principal-plane pattern cuts at $f=f_0$.

To round-out the analyses of these antennas presented so far, we provide images of the predicted 3D far-field patterns, at five frequencies {0.9x, 0.95x, 1.0x, 1.05x, and 1.1x} f_0, for each of the aforementioned antennas, in the figures that fill the following four pages. Note that *unlike* the polar patterns in Figure 17, the gain plot ranges (min to max scale) of the 3D patterns that follow are not all the same; the reader is cautioned to use care when comparing different plots.

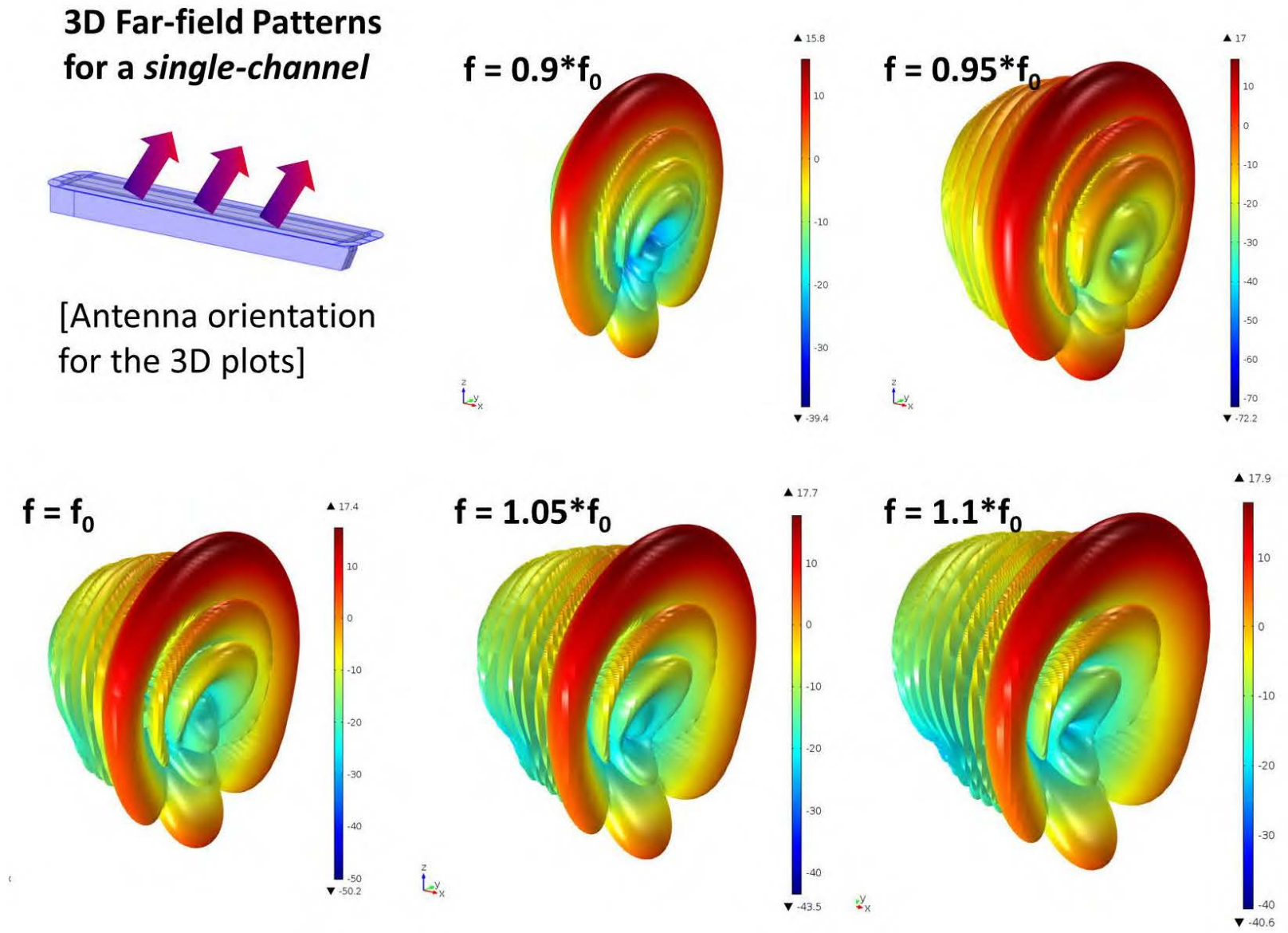

Figure 18. Selected 3D far-field patterns for a single-channel FAWSEA.

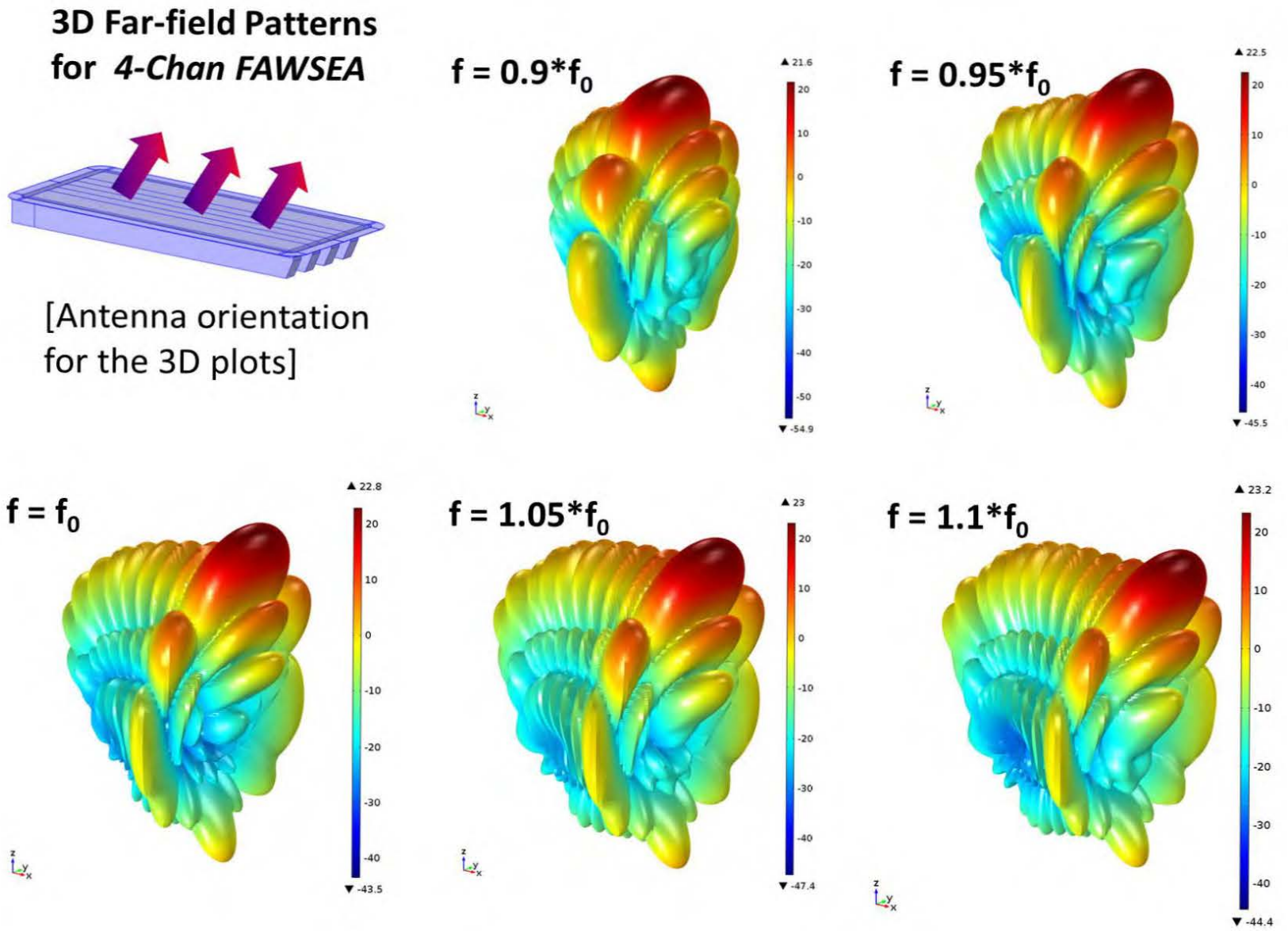

Figure 19. Selected 3D far-field patterns for a four-channel FAWSEA.

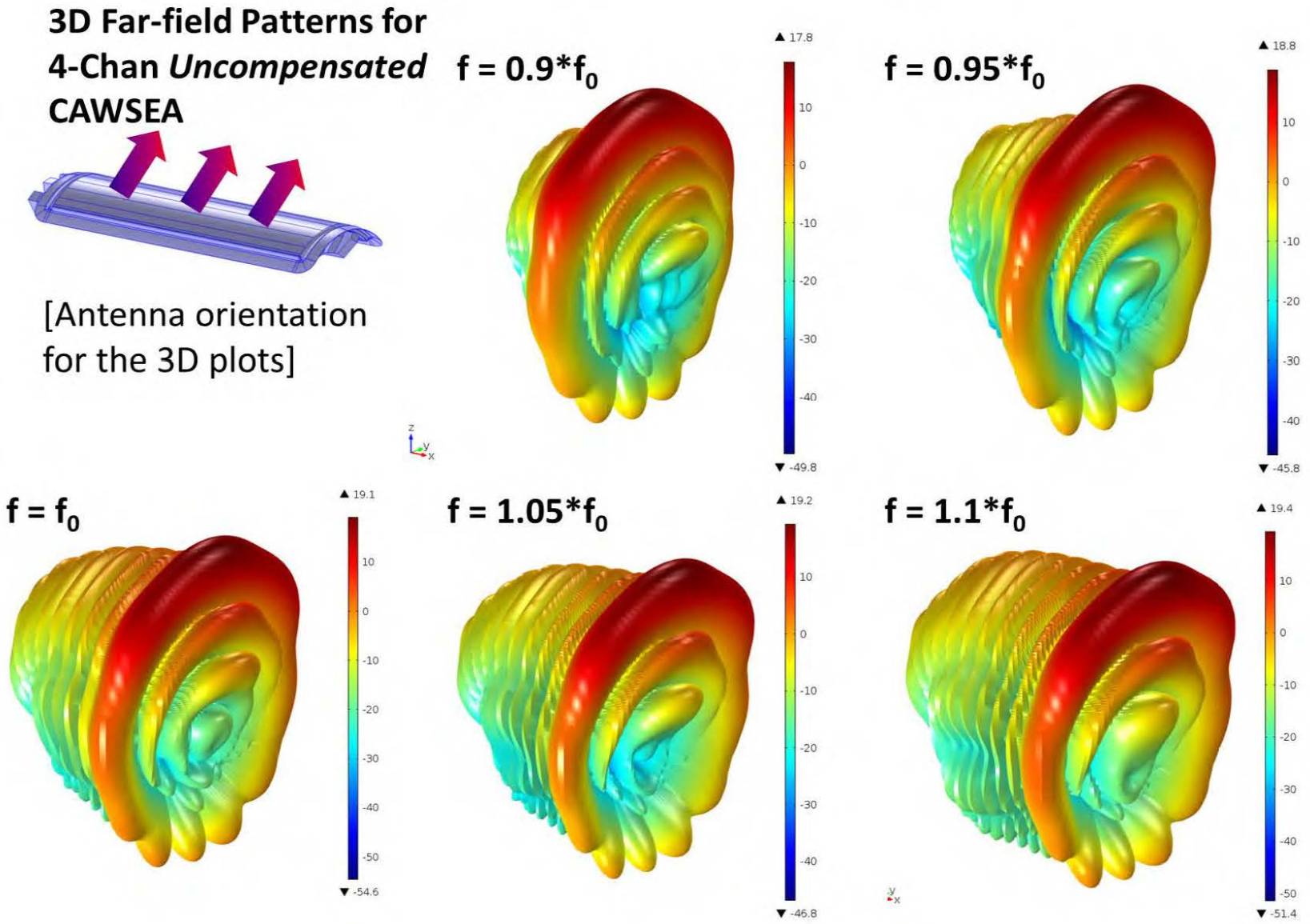

Figure 20. Selected 3D far-field patterns for a four-channel *uncompensated* CAWSEA.

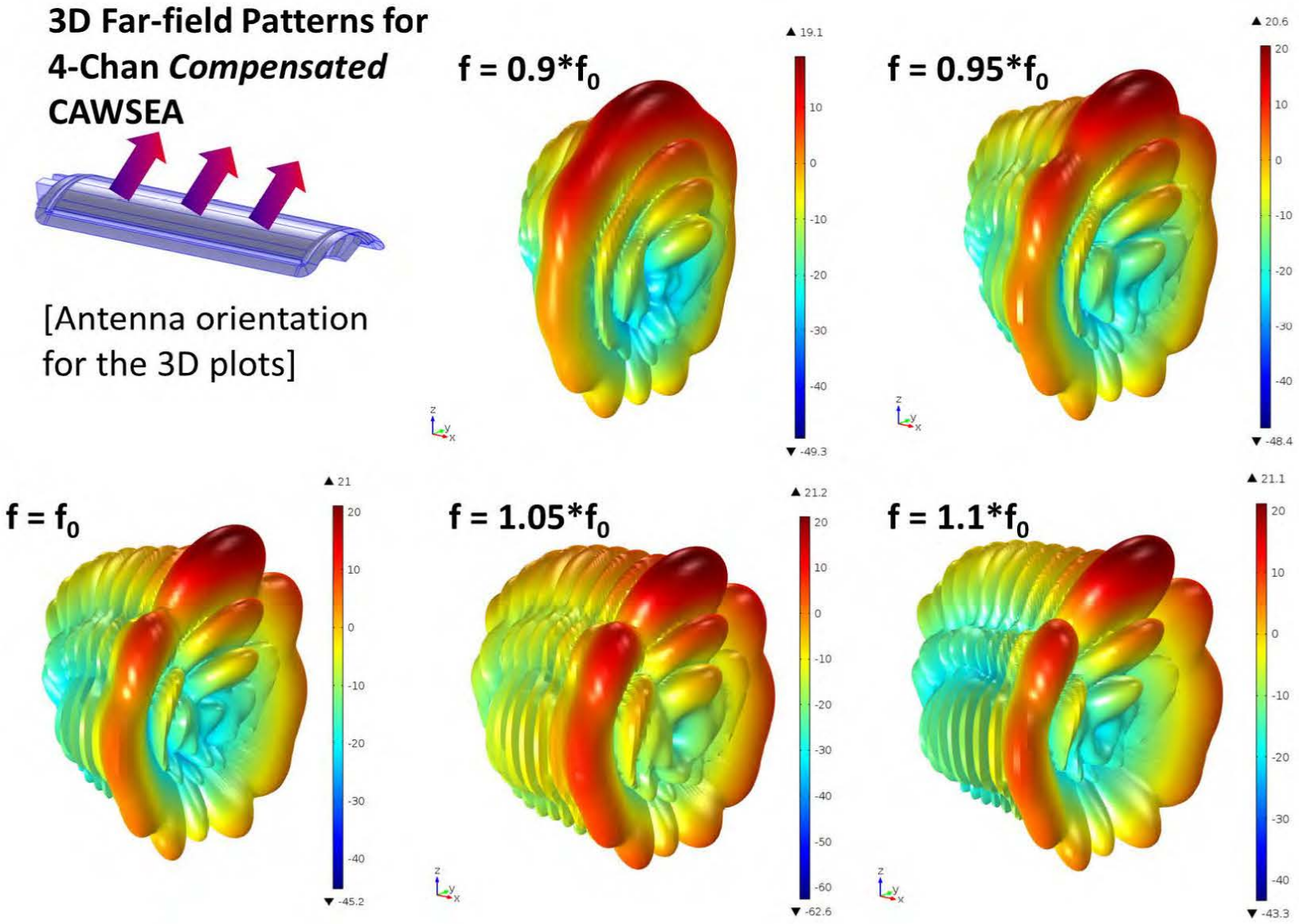

Figure 21. Selected 3D far-field patterns for a four-channel CAWSEA compensated at $f=f_0$.

4. DISCUSSION, CONCLUSIONS, AND RECOMMENDATIONS

As planned, work performed during this 5th quarter of the R&D program led us to document the specific designs (for FAWSEA and CAWSEA) presented in this report, which exemplify practical, realistic, high-performance, wavelength-scalable, configurations of this antenna technology.

In the coming quarter, we look forward to further extending/applying the theory established to date to the additional aperture types noted in the 4th report, and to documenting additional, representative, high-performance designs. As always, we appreciate ONR's continuing support for this R&D.

BIBLIOGRAPHY (alphabetical)

Goldstone, L.O. and Oliner, A.A., "Leaky-Wave Antennas I: Rectangular Waveguides," *IRE Trans. Ant. and Propagat*., Oct., 1959, pp. 307-319.

Goldstone, L.O. and Oliner, A.A., "Leaky-Wave Antennas II: Circular Waveguides," *IRE Trans. Ant. and Propagat*., May., 1961, pp. 280-290.

Honey, R.C., "A Flush-Mounted Leaky-Wave Antenna with Predictable Patterns," *IRE Trans. Antennas and Propagat*., 7, pp. 320-329, 1959.

Ishimaru, A.K. and Beich, F.R., "Pattern Synthesis With a Flush-Mounted LeakyWave Antenna on a Conducting Circular Cylinder," *J. of Res. of the Nat. Bureau of Standards-D. Radio Propagat* Vol. 66D, No.6, Nov- Dec. 1962, pp. 783-796.

Jull, E.V., "Radiation from Apertures," Chap. 5 of *Antenna Handbook: Theory, Applications, and Design,* Ed. by Y.T. Lo and S.W. Lee, Van Nostrand Reinhold, NY, 1988.

Marcuvitz, N., *Waveguide Handbook*, McGraw-Hill, NY, 1951.

Nishida, S., "Coupled Leaky Waveguides I: Two Parallel Slits in a Plane" *IRE Trans. Ant. and Propagat*., May, 1960, pp. 323-330.

Nishida, S., "Coupled Leaky Waveguides II: Two Parallel Slits in a Cylinder," *IRE Trans. Ant. and Propagat.,* July, 1960, pp. 354-360.

Oliner, A.A. and R.G. Malech, "Radiating Elements and Mutual Coupling," "Mutual Coupling in Infinite Scanning Arrays," and "Mutual Coupling in Finite Scanning Arrays," -- Chaps. 2, 3, and 4 respectively of *Array Theory and Practice*, Vol. II of *Microwave Scanning Antennas*, Ed. by R.C. Hansen, Peninsula Publishing, Los Altos, CA, 1985.

Oliner., A.A, and D.R. Jackson, "Leaky Wave Antennas," Chap. 11 of *Antenna Engineering Handbook*, 4th Ed., Edited by J.L. Volakis, McGraw-Hill, NY, 2007.

Silver, S., *Microwave Antenna Theory and Design,* 1st Ed, publ. by office of Scientific Research and Development, National Defense Research Committee, NY, 1949.

SUGGESTED DISTRIBUTION LIST

Official Record Copy
Mr. Lee Mastroianni
E-Mail: lee.mastroianni@navy.mil
Code 30
Office of Naval Research
875 North Randolph St.
Arlington, VA 22203-1995 1 cy

Dr. Joong H. Kim
E-Mail: joong.kim@navy.mil
Code 30
Office of Naval Research
875 North Randolph St.
Arlington, VA 22203-1995 1 cy

Director, Naval Research Lab
E-mail: reports@library.nrl.navy.mil
Attn: Code 5596
4555 Overlook Avenue, SW
Washington, D.C. 20375-5320 1 cy

Defense Technical Information Center
E-mail: tr@dtic.mil
8725 John J. Kingman Road
STE 0944
Ft. Belvoir, VA 22060-6218 1 cy

Dr. Donald Shiffler
AFRL/RDH
Kirtland AFB, NM 87117-5776 1 cy

Dr. Michael Haworth
AFRL/RDHP
Kirtland AFB, NM 87117-5776 1 cy

Dr. Andrew D. Greenwood
AFRL/RDHE
Kirtland AFB, NM 87117-5776 1 cy

Dr. Susan Heidger
AFRL/RDH
Kirtland AFB, NM 87117-5776 1 cy

Matthew McQuage
Naval Surface Warfare
Dahlgren Division 1 cy

Michael Wagaman
Advanced Technology Directorate
PEO Strike Weapons and Unmanned Aviation
Patuxent River, MD. 1 cy

Dr. Frank E. Peterkin
Director
Directed Energy Technology Office
Dahlgren, VA 1 cy

LTC Chuck Ormsby
Chief
Directed Energy Requirements
Langley AFB, VA 1 cy

Patrick Randeson
Science, Technology and Weapons Analyst
Central Intelligence Agency
Washington, D.C. 1 cy